Vegetation dynamics and its driving forces from climate change and human activities in the Three-River Source Region, China from 1982 to 2012

Ying Zhang [a], Chaobin Zhang [a], Zhaoqi Wang [a], Yizhao Chen [a], Chengcheng Gang [a], Ru An [b], Jianlong Li [a,*]

[a] School of Life Science, Nanjing University, Xianlin Road 163, Qixia District, Nanjing, 210046, China
[b] School of Earth Science and Engineering, Hohai University, Xikang Road 129, Nanjing, 210098, China

HIGHLIGHTS

- Partitioned the contributions of human activities and climate change to NPP trends.
- The relationships of different climate factors and NPP were analyzed quantitatively.
- Radiation was the most important climate factor of NPP interannual variation.
- After 2001, the climate conditions changed from benefit for vegetation to negative.
- Whereas the effect of human activities changed from negative to positive after 2001.

ARTICLE INFO

ABSTRACT

The Three-River Source Region (TRSR), a region with key importance to the ecological security of China, has undergone climate changes and a shift in human activities driven by a series of ecological restoration projects in recent decades. To reveal the spatiotemporal dynamics of vegetation dynamics and calculate the contributions of driving factors in the TRSR across different periods from 1982 to 2012, net primary productivity (NPP) estimated using the Carnegie–Ames–Stanford approach model was used to assess the status of vegetation. The actual effects of different climatic variation trends on interannual variation in NPP were analyzed. Furthermore, the relationships of NPP with different climate factors and human activities were analyzed quantitatively. Results showed the following: from 1982 to 2012, the average NPP in the study area was 187.37 g cm^{-2} yr^{-1}. The average NPP exhibited a fluctuation but presented a generally increasing trend over the 31-year study period, with an increase rate of 1.31 g cm^{-2} yr^{-2}. During the entire study period, the average contributions of temperature, precipitation, and solar radiation to NPP interannual variation over the entire region were 0.58, 0.73, and 0.09 g cm^{-2} yr^{-2}, respectively. Radiation was the climate factor with the greatest influence on NPP interannual variation. The factor that restricted NPP increase changed from temperature and radiation to precipitation. The average contributions of climate change and human activities to NPP interannual variation were 1.40 g cm^{-2} yr^{-2} and -0.08 g cm^{-2} yr^{-2}, respectively. From 1982 to 2000, the general climate conditions were favorable to vegetation recovery, whereas human activities had a weaker negative impact on vegetation growth. From 2001 to 2012, climate conditions began to have a negative impact on vegetation growth, whereas human activities made a favorable impact on vegetation recovery.

© 2016 Elsevier B.V. All rights reserved.

1. Introduction

Net primary productivity (NPP) is originally defined as the amount of photosynthetically fixed carbon available to the first heterotrophic level in an ecosystem (Field et al., 1998). NPP is an indicator of the extent of vegetation light utilization under natural conditions (Yu et al., 2009). It is also an important indicator of the health and ecological balance of an ecosystem, as well as a key element for assessing carbon sink and ecological regulatory behavior (Gao et al., 2009). A decline in vegetation productivity is the major manifestation of vegetation degradation, whereas NPP is an important indicator of productivity. In recent years, many studies of NPP have been conducted in recent years (Nemani et al., 2003; Hein et al., 2011; Mu et al., 2013a; Zhou et al., 2015; Wu et al., 2014; Yang et al., 2014), which explored the long-term monitoring of vegetation dynamics in terrestrial ecosystems, on

---

* Corresponding author.
E-mail addresses: lijianlongnju@163.com, jlli2008@nju.edu.cn (J. Li).

both local and global scales. Terrestrial ecosystems are susceptible to the combined effects of climate conditions and human activities (Esser, 1987; Haberl, 1997). With aggravating global climate change and increasing human activities (Vitousek, 1994; IPCC, 2007), quantifying the influence of different driving factors on vegetation dynamics has become an important issue to formulate countermeasures and management policies. To date, several efforts have been devoted to separately quantify the influence of climatic and anthropogenic factors on an ecosystem within a specific region (Wessels et al., 2004; Wu et al., 2014; Mu et al., 2013a, 2013b; Nayak et al., 2013; Chen et al., 2014).

China is currently confronted by severe grassland degradation (Akiyama and Kawamura, 2007; Harris, 2010). A series of policies that addressed this problem was launched in the early 21st century, such like the Grain to Green Program (GTGP, which is usually explained as "replacing cropping and livestock grazing in fragile areas with trees and grass") and the Grazing Withdrawal Program (GWP, which is aimed to conserve grassland through banning of grazing, rotational grazing or converting grazing land to cultivated pasture) (Wang et al., 2007b; Liu et al., 2008a; Mu et al., 2013b). The effect of such policies became a major concern of the society. The Three-River Source Region (TRSR), which lies in the hinterland of the Tibetan Plateau, is dominated by natural grasslands (Chang et al., 2014). The region is not only an important ecological barrier of China, but it also has a sensitive and fragile ecological environment (Liu et al., 2014). In the past decades, the TRSR has attracted considerable attention because of its grassland degradation problem (Liu et al., 2008b; Wang et al., 2009; Liu et al., 2014). The climate conditions and human activities in this region have obviously changed. For the past decades, the TRSR has suffered from climate warming, which has been aggravated in the 21st century. Since the national nature reserve was designated in the TRSR in the early 21st century, a series of ecological protection policies and projects has been implemented in this area (Fang, 2013; Tong et al., 2014). However, only a few studies have been conducted to quantitatively analyze the relationships of vegetation growth with climate factors and human activities in the TRSR (Qian et al., 2010; Liu et al., 2014), particularly to compare the differences in such relationships across different periods or to distinguish the effects of various climate factors.

Therefore, this study attempts to accurately simulate the spatiotemporal evaluation of the dynamics of vegetation NPP in the TRSR for the past 31 years (1982–2012) and to distinguish the effects of various driving factors on vegetation dynamics. The NPP in the TRSR is estimated by the Carnegie–Ames–Stanford approach (CASA) model and used as an indicator of vegetation dynamics. Furthermore, the spatiotemporal dynamics of vegetation NPPs across different periods of the 21st century are analyzed. The cumulative effects of different driving factors on NPP interannual variation are determined. Our aim is to provide an accurate method for evaluating the health status of the vegetation conditions in the TRSR and the effects of ecosystem protection projects. The findings can be used to promote sustainable utilization, ecological construction, and policy formulation in the TRSR.

2. Materials and methods

2.1. Study area

The TRSR is the headstream of three major rivers (i.e., the Yangtze River, the Yellow River, and the Lantsang River) in East Asia, and around 40% of the world's population depends on, or is influenced by these rivers (Foggin, 2008). The TRSR covers an area of 350,000 km^2, of which the source region of the Yangtze River is 150,000 km^2, that of the Yellow River is 90,000 km^2, and that of the Lantsang River is 30,000 km^2. The area of other inland river basins is 60,000 km^2. The original natural vegetation and the soil rich in organic matter in the TRSR fulfill significant water conservation functions. This region supplies 25% of the total water of the Yangtze River, 49% of the total water of the Yellow River, and 15% of the total water of the Lantsang River (Zhang et al., 2012).

Thus, the TRSR is known as the "Water Tower of China". The TRSR is mainly constituted of mountainous landforms with altitudes ranging from 3335 m to 6564 m. The major mountains include the East Kunlun Mountain and its branch the Aemye Machhen Range, the Bayan Har Mountain, and the Tanggula Mountain. This region features a fluctuating terrain, dense river networks, numerous rivers, extensive snowy mountains, and crisscrossing glaciers. The TRSR has a typical high-altitude continental climate, with small annual temperature difference, large diurnal temperature range, and a notably decreasing trend of heat and water from southeast to northwest. The growing season in this region is from May to September. The population is approximately 568,000, and most of the residents are Tibetan with a nomadic lifestyle (Harris, 2010). The grassland is the primary ecosystem in the TRSR. The main grassland types are alpine meadow and alpine steppe (Fan et al., 2010). As mentioned in Section 1, the TRSR has attracted considerable attention in the past decades because of its grassland degradation problem. With a deteriorating regional ecosystem and a decline in water conservation function, the life of the residents in this region is threatened. In addition, the ecological security of the Yangtze River basin, the Yellow River basin, and even the Southeast Asia region is in danger.

2.2. Data source and processing

2.2.1. Climate data

The climate data used in this study are the 1982–2012 data on monthly average temperature, monthly precipitation, solar radiation, and altitude from 50 standard weather stations in the TRSR and its surrounding area, which are provided by the Meteorological Data Sharing Service System of China. This data was interpolated by using ANUSPLIN version 4.2 software to regular monthly data layers with the spatial resolution same as NDVI data. Given the fluctuating terrain and sparse meteorological stations in the TRSR, common interpolation methods cannot achieve high precision (Li et al., 2003), thus, interferences to NPP calculation and data analysis are introduced as subsequent treatments. To solve this problem, ANUSPLIN (a software program developed by the Australian National University for the spatial interpolation of climate data using a thin plate smoothing spline) (Hutchinson, 2001), is used in this study for interpolation. It has been proved be more appropriate for spatial interpolation of climate than other methods in the TRSR (Peng et al., 2010).

2.2.2. Remote sensing data

To create a long time series of NDVI data set from 1982 to 2012, two kinds of NDVI sources are used. The NDVI data of 1982–2000 are the Global Inventory Modeling and Mapping Studies (GIMMS) NDVI data produced by the Global Land Cover Facility of the University of Maryland, with an original spatial resolution of 8 km. During the preparation of this data set, its creators performed radiation correction, geometric correction, and cloud filtering to improve data accuracy. In our study, the GIMMS–NDVI data are resampled to have a spatial resolution of 1 km. Meanwhile, the remote sensing data of 2001–2012 are the MODIS 13A2 data, with a spatial resolution of 1 km. The MODIS–NDVI data are subjected to format conversion and reprojection in our study; spatial splicing and resampling are also performed. Using the 16-d MODIS–NDVI data, monthly NDVI data are obtained via the maximum-value composite (MVC) procedure.

Using the Spector–Grant filtering method, which is a denoising technique for NDVI data, the two types of NDVI data are smoothed and filtered. Given that the two types of MODIS data by GIMMS are acquired using different sensors, conducting a consistency test between them is necessary. The two types of data overlap in 84 months (2000–2006). A correlation analysis of the monthly average NDVI indicates that the correlation coefficient is 0.87 (P < 0.001). Thus, the two types of data are significantly consistent at the regional scale. The linear regression equation between the two types of data for each pixel is established using the recursive least square method with the overlapped data, and the average R^2 of all pixels is 0.84 (P < 0.001). The GIMMS–NDVI data

of 2001–2012 are interpolated. The time of data is prolonged to finally obtain the raster images of the monthly NDVI of 1982–2012 in the TRSR.

2.2.3. Data on vegetation types

Data on vegetation types are from the Global Land Cover 2000 data set (GLC 2003) with a spatial resolution of 1 km.

2.2.4. Measurement data

Given that NPP measurement is difficult, NPP data converted from biomass are typically used to replace the measured NPP for model validation. The biomass data measured at 50 plots with dimensions of 1 km × 1 km in the TRSR in August 2012 are selected. The area of a quadrate is 1 m × 1 m, with 5 replicates. The aboveground part is harvested, and the sample is dried at 70 °C in a thermostatic oven until a constant weight is achieved as the above-ground dry matter. According to the study of Wu et al. (2010) on the carbon flux of meadows in the Tibetan Plateau, a carbon distribution ratio of 58.7:41.3 between the underground and aboveground parts is selected. The observed NPP is obtained using the following equation:

$$NPP = DM_{AG}(1 + 58.7/41.3) * 0.542 \qquad (1)$$

where DM_{AG} is the above-ground dry matter, and 0.542 accounts for the carbon conversion rate of grassland (Zhu et al., 2007).

2.3. Methods

2.3.1. Calculating NPP and interannual variation rate

The NPP in the TRSR is calculated using the CASA model, which is a process-based model driven by remote sensing and climate data (Potter et al., 1993; Field et al., 1995). In the CASA model, NPP is the product of absorbed photosynthetically active radiation (APAR) and the utilization efficiency (ε) of vegetation on APAR that reaches the surface (Potter et al., 1993). It is expressed as follows:

$$NPP(x, t) = APAR(x, t) \times \varepsilon(x, t), \qquad (2)$$

where x is the spatial location (pixel number), and t is the time. $APAR(x,t)$ represents the canopy-absorbed incident solar radiation of pixel x in t time (MJ m^{-2}), and $\varepsilon(x,t)$ represents the actual light-use efficiency (g C MJ^{-1}) of pixel x in t time.

$APAR(x,t)$ is calculated as follows:

$$APAR(x, t) = SOL(x, t) \times FPAR(x, t) \times 0.5, \qquad (3)$$

where $SOL(x,t)$ is the total solar radiation (MJ m^{-2}) of pixel x in t time; and $FPAR(x,t)$ is the fraction of photosynthetically active radiation absorbed by the vegetation canopy, which can be determined by NDVI (Ruimy et al., 1994). The value of 0.5 denotes the fraction of the total solar radiation that is available for vegetation (0.38–0.71 μm).

$\varepsilon(x,t)$ may be calculated as follows:

$$\varepsilon(x, t) = T\varepsilon_1(x, t) \times T\varepsilon_2(x, t) \times W\varepsilon(x, t) \times \varepsilon_{\max}, \qquad (4)$$

where $T\varepsilon_1(x,t)$ and $T\varepsilon_2(x,t)$ are the temperature stress coefficients, which reflect the reduction in light-use efficiency caused by a temperature factor (Potter et al., 1993; Field et al., 1995). $W\varepsilon(x,t)$ is the moisture stress coefficient, which indicates the reduction in light-use efficiency caused by a moisture factor. $\varepsilon_{\max}$ is the maximum ε under ideal conditions set as different constant parameters for various vegetation types (Zhu et al., 2007): grassland (0.542), bush (0.429), evergreen needle-leaf forest (0.389), and others (0.542). A more detailed description of the model is provided by Yu et al. (2011).

2.3.2. Interannual variation rate of NPP

A simple linear regression is employed to analyze the interannual variation in vegetation NPP in the TRSR from 1982 to 2012. The slope

of the trend line in the multi-year regression equation for a single pixel represents the interannual variation rate, which is solved by the least squares method as follows:

$$\theta slope = \left(n \times \sum\nolimits_{i=1}^{n} i \times NPP_i - \left(\sum\nolimits_{i=1}^{n} i \right) \left(\sum\nolimits_{i=1}^{n} NPP_i \right) \right) \\ / \left(n \times \sum\nolimits_{i=1}^{n} i^2 - \left(\sum\nolimits_{i=1}^{n} i \right)^2 \right) \qquad (5)$$

where $\theta slope$ is the interannual variation rate of NPP, n is the number of years simulated, and NPP_i is the vegetation NPP in the ith year. The correlation between NPP sequences and time sequences (year) is used to determine the significance of interannual variation in NPP. A negative slope indicates a decreasing trend, whereas a positive slope indicates an increasing trend.

The significance of the variation tendency is determined using the F test to represent the confidence level of variation. The calculation formula for statistics is expressed as follows:

$$F = U \times (n-2)/Q \qquad (6)$$

where $Q = \sum_{i=1}^{n}(y_i - \hat{y}_i)$ and is the sum of the square error, $U = \sum_{i=1}^{n}(\hat{y}_i - \overline{y})^2$ and is a regression sum of the squares. y_i is the observed NPP in the ith year, and $\hat{y}_i$ is the regression value; $\overline{y}$ is the mean NPP over the years, and n is the number of years studied.

2.3.3. Contribution of each driving factor to interannual variation in NPP

NPP variation is the function of climate (mainly refers to temperature, precipitation, and solar radiation) and other variables (mainly refers to human activities); thus, the contribution of each factor to the interannual variation rate of NPP can be estimated for each pixel using Eq. (7). Similar methods based on partial derivatives are now widely used in studies on the effects of climate on hydrological dynamics (Rana and Katerji, 1998; Meng and Mo, 2012; Yang and Yang, 2012).

$$\begin{aligned} \theta slope &= C(tem) + C(rad) + C(pre) + UF \\ &= (\partial NPP/\partial tem) \times (\partial tem/\partial n) + (\partial NPP/\partial rad) \times (\partial rad/\partial n) \\ &\quad + (\partial NPP/\partial pre) \times (\partial pre/\partial n) + UF \end{aligned} \qquad (7)$$

where $\theta slope$ is the interannual variation rate of NPP, which is solved in Eq. (5). The average temperature, solar radiation, and precipitation during the growth season of the TRSR are denoted by tem, rad, and pre, respectively. The growth season of this region is from May to September. The time delay effect between climate factors and vegetation indices in this region, the average temperature from April to September, and the precipitation and total solar radiation from May to September used in this study are drawn from An et al. (2014). $C(tem)$, $C(rad)$, and $C(pre)$ are the contributions of tem, rad, and pre to the interannual variation rate of NPP; and n is the number of years simulated. $C(tem)$ can be calculated as $(\partial NPP/\partial tem)$, which is the slope of the linear regression line between NPP and tem, and $(\partial tem/\partial n)$ is the slope of the linear regression line between tem and n. $C(rad)$ and $C(pre)$ are calculated in the same manner. UF is the residual between the variation rates of NPP and climate factor contribution; it represents the variation rate of the contribution of unknown factors to NPP. Both human factors and some uncertain natural factors (such as natural disaster, wind, et al.) are contained in UF, and we suppose that the former takes a dominant position.

2.3.4. Validating NPP

Correlation analysis is performed between NPP simulated by the CASA model and the measured NPP. The results (Fig. 2) exhibit good correlation between measured and simulated NPPs ($R^2 = 0.6993$, $P < 0.001$). Thus, the result of the model simulation is reliable. (See Fig. 1.)
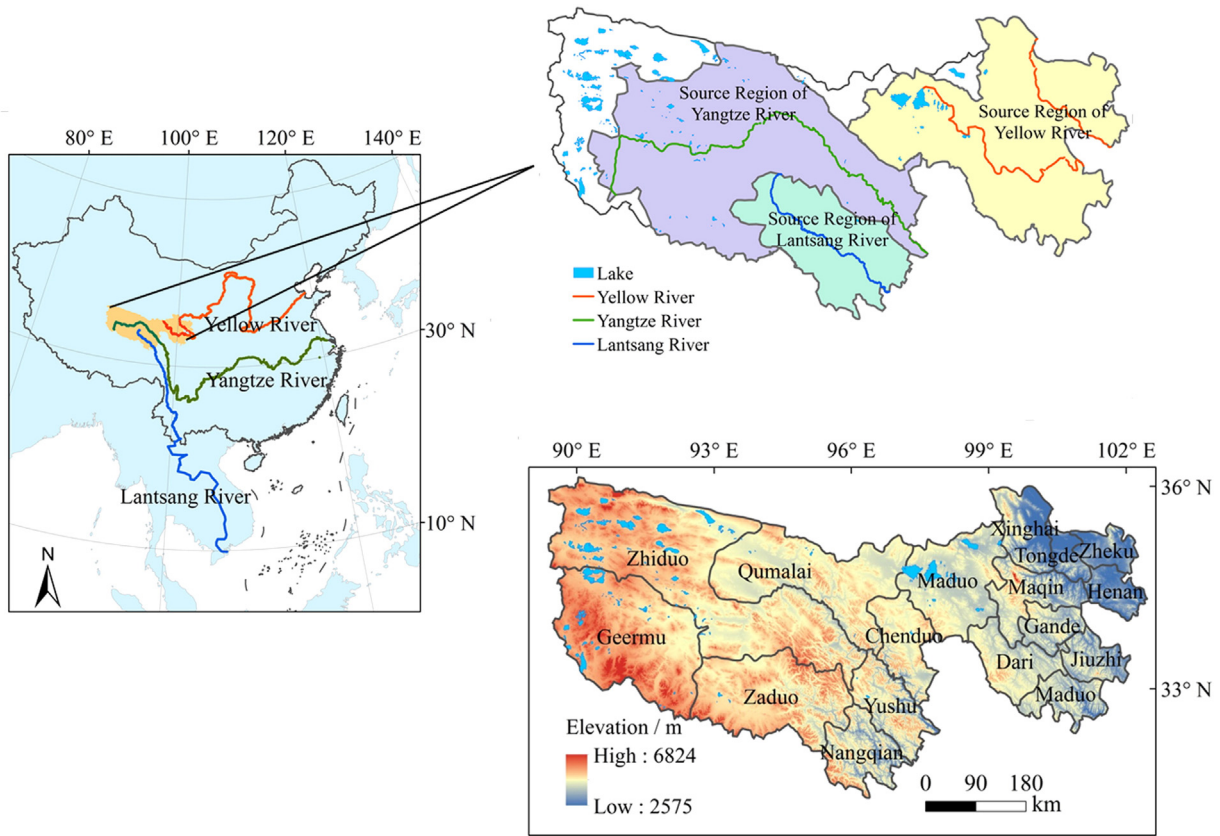
Fig. 1. Location of the study area and its subregions.

3. Results

3.1. Spatiotemporal pattern of NPP

The spatial distribution variation in NPP is large over the entire TRSR (Fig. 3). The average vegetation NPP from 1982 to 2012 is 187.37 g cm^{-2} yr^{-1}, and the total NPP is 59.43 Tg C yr^{-1}. NPP decreases gradually from southeast to northwest, which conforms to the distribution of the hydrothermal gradient in the TRSR. NPP is higher in Zeku County and Henan County to the east of 100° E and in Yushu County to the south of the TRSR, with values typically within the range of 300–400 g cm^{-2} yr^{-1}. NPP is lower in Ge'ermu County to the west of

Fig. 2. Comparison between simulated and measured NPPs in the TRSR.

94° E and in the northwest of Zaduo County, with values within the range of 20–100 g cm^{-2} yr^{-1}.

The average and total NPPs in the source regions of the Yangtze River, the Yellow River, and the Lantsang River are calculated. NPP is highest in the source region of the Yellow River, with an average value of 269.20 g cm^{-2} yr^{-1} and a total value of 21.08 Tg; the average NPP in the source region of the Lantsang River is 231.78 g cm^{-2} yr^{-1} and the total NPP is 9.05 Tg; lastly, the NPP in the source region of the Yangtze River is the lowest, with an average value of 160.40 g cm^{-2} yr^{-1} and a total value of 21.08 Tg.

As shown by the interannual variation in average NPP over the entire region from 1982 to 2012 (Fig. 4), the highest NPP in 31 years is generated in 1994 (217.83 g cm^{-2} yr^{-1}), whereas the lowest NPP is generated in 1989 (152.46 g cm^{-2} yr^{-1}). The seasonal and annual variations in average NPP of the entire region are significant, with amplitudes ranging from 0.2% to 18.6%. At the 31-year time scale, the increase rate of average NPP over the entire region is 1.31 g cm^{-2} yr^{-2} (P < 0.01). The increase is rapid during the first 19 years (1.99 g cm^{-2} yr^{-2}, P < 0.01). However, after entering the 21st century, the NPP exhibits an insignificant decreasing trend (−0.24 g cm^{-2} yr^{-2}).

The variations in NPP present apparent differences across three time scales (Fig. 5).

In 1982–2000 (Fig. 5a), the regions with extremely significant or significant increase in NPP are mainly distributed in Maqin County, Gande County, and Maduo County, which are to the east of the TRSR. Such increase can also be observed in Ge'ermu City in the west and in north Zaduo County. However, NPP does not change significantly in the extensive area in the middle of the TRSR.

In 2001–2012 (Fig. 5b), the regions with a decrease in NPP are distributed in Tongde County, Maqin County, and Gande County in the east, as well as Yushu County, Chengduo County, and Nangqian County in the south. The regions with an increase in NPP are concentrated in
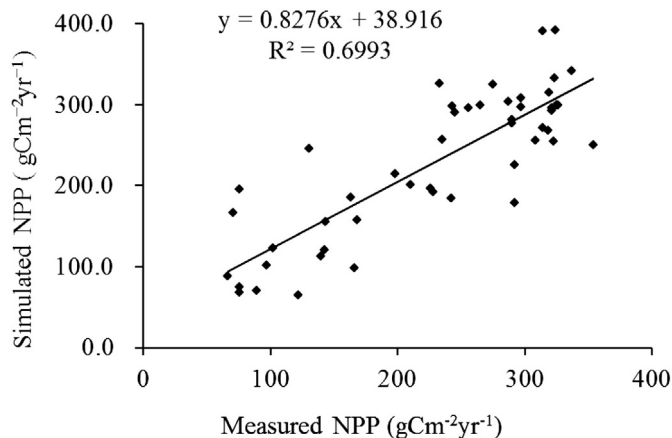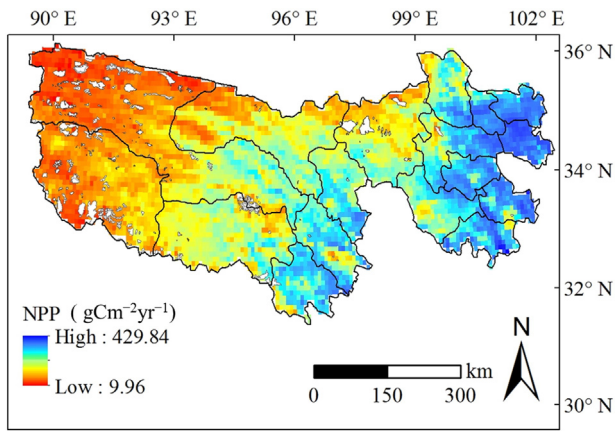
Fig. 3. Spatial distribution of mean NPP in the TRSR from 1982 to 2012.

Zaduo County and Ge'ermu County in the northwest, as well as in some parts of Maduo County and Xinghai County in the north.

At the 31-year time scale (Fig. 5c), the vegetation NPP in the TRSR exhibits a generally increasing trend. The regions with an extremely significant increase, a significant increase, an insignificant variation, a significant decrease, and an extremely significant decrease in NPP account for 49.09%, 13.78%, 36.32%, 0.56%, and 0.24% of the total area, respectively. The regions with an extremely significant increase in NPP account for the largest proportion. The dense distribution is mainly found in the east of 97.5° E and also in other parts of the TRSR. The regions with a significant decrease and an extremely significant decrease in NPP account for only a very small proportion, and the distribution is sporadic.

The NPP variations across the three source regions at three time scales are calculated (Fig. 6). At the 31-year time scale, the vegetation NPP across all three source regions exhibits a generally increasing trend. The area with an increase in NPP is the largest in the source region of the Yellow River (79.37%). Meanwhile, the areas with an increase in NPP in the source regions of the Yangtze River (55.92%) and the Lantsang River (56.07%) are very similar. The proportions of areas with NPP decrease are all small across the three source regions. Before the 21st century, the area with an increase in NPP also accounts for the largest proportion in the south region of the Yellow River. The proportions are similar in the source regions of the Yangtze River and the Lantsang River. However, for most parts of the three source regions, the variation in NPP is insignificant, and nearly no region exhibits a significant decrease in NPP. After the 21st century, the proportions of areas with an increase in NPP all decrease considerably across the three source regions; by contrast, the proportions of areas with a reduction in NPP rise markedly. The proportion of areas with a decrease in NPP is largest in the source region of the Lantsang River (25.98%), followed by that of the Yangtze River (18.65%).
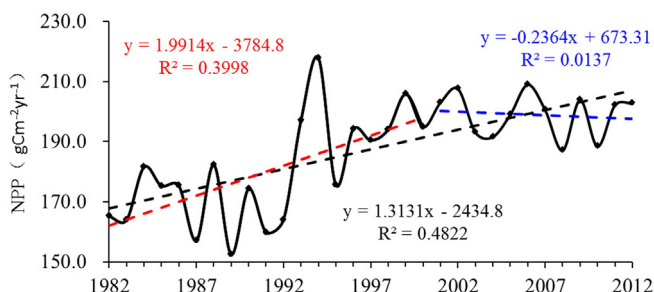

Fig. 4. Dynamics of annual NPP in the TRSR.

3.2. Quantitative analysis of driving factors of interannual variation in NPP in the TRSR

3.2.1. Correlations between NPP and climate factors

Correlation analysis is performed between each climate factor and the simulated NPP during the growth season. One point to note is that this analysis is closely related to the NPP model and climate interpolation method. Over the entire TRSR, the correlation coefficients of temperature, precipitation, and radiation to NPP in 31 years are 0.22, 0.07, and 0.46, respectively ($P < 0.05$). The correlation coefficients of NPP to each climate factor in the three source regions are calculated (Fig. 7). A significant difference is observed before and after the 21st century. After 2001, the positive correlations between NPP and temperature in the three source regions all decrease compared with those before 2001. NPP is negatively correlated with precipitation in the source regions of the Yangtze River (Fig. 7a) and the Yellow River (Fig. 7b) before 2001. Afterward, the two are either positively correlated or negatively correlated to a smaller extent. For the source region of the Lantsang River (Fig. 7c), the positive correlation between NPP and precipitation before 2001 changes into a negative correlation. After 2001, the positive correlation between temperature and NPP in the TRSR has weakened, whereas their negative correlation has become enhanced. By contrast, the positive correlation between precipitation and NPP has become enhanced, whereas their negative correlation has weakened. These results indicate that the factor that restricts the growth of NPP in the TRSR has changed from temperature and radiation to precipitation.

3.2.2. Contributions of climate factors to interannual variation in NPP

The correlation coefficient characterizes the degree of correlation between NPP and each climate factor. However, it cannot quantify the influence of each climate factor on seasonal and annual variations in NPP. To quantify the influence of each climate factor on interannual variation in NPP, the contribution of each driving factor to interannual variation in NPP is used to analyze the relationship of NPP to each climate factor and human activity. The differences in various periods are compared and shown in Fig. 8.

During the growth season of 1982–2000 (top row of Fig. 8), the three climate factors mainly make positive contributions to NPP in most parts of the TRSR. The regions with the highest contribution are located in the east of the source region of the Yellow River. The average contributions of temperature, precipitation, and radiation to NPP over the entire region are 0.75, 0.14, and 1.57 g cm^{-2} yr^{-2}, respectively. Radiation makes the greatest contribution to NPP trend among all climate factors.

The period of 2001–2012 (middle row of Fig. 8) experiences an obvious change from the situation 19 years ago. The three climate factors make negative contributions to NPP trend in most parts of the TRSR. The average contributions of temperature, precipitation, and radiation to NPP over the entire region are −0.05, −0.21, and −0.51 g cm^{-2} yr^{-2}, respectively. Solar radiation makes the greatest negative contribution to NPP trend, and temperature makes the smallest negative contribution.

At the 31-year time scale (bottom row of Fig. 8), temperature seems to always make a strong positive contribution to NPP over the entire region. Precipitation makes a strong positive contribution in the west of the source regions of the Yellow River and the Yangtze River. The average contributions of temperature, precipitation, and radiation to NPP over the entire region are 0.58, 0.73, and 0.09 g cm^{-2} yr^{-2}, respectively. Solar radiation makes a strong positive contribution in the southeast of the TRSR and a gradually increasing negative contribution in the northwest. Over the entire TRSR, all three climate factors make positive contributions to NPP trend. Solar radiation makes the strongest contribution, followed by temperature, whereas precipitation makes a considerably weaker contribution.

To analyze the actual effects of different climatic variation trends on interannual variation in NPP, we combine the partial correlation coefficient and climate contributions of each climate factor to NPP. Table 1
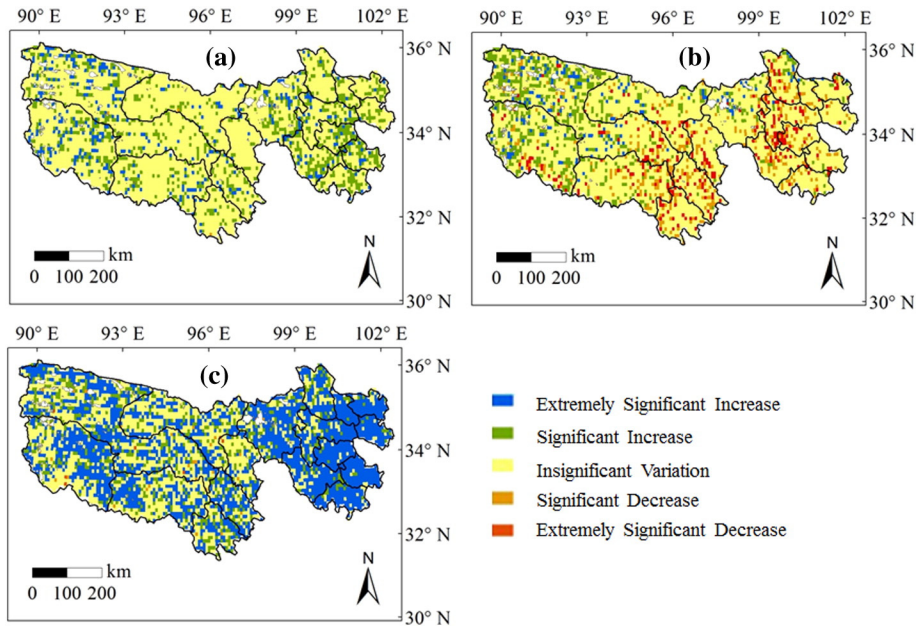
Fig. 5. Gradation rate of the significance of variations in NPP in the TRSR in (a) 1982–2000, (b) 2001–2012, (c) and 1982–2012.

presents the 12 combinations of partial correlation coefficients and climate contributions to NPP trend.

The proportions of areas with each combination before and after 2001 are calculated (Fig. 9). In 1982–2000, the area of Sol_sp_c+ is the largest, reaching 55.86%. These regions are mainly distributed in the east and south of the TRSR. The area with Tem_sp_c+ and Tem_sn_c− also account for small proportions (1.72% and 1.58%, respectively). In 2001–2012, the area of Sol_sp_c− is the largest (8.93%), and the regions with Sol_sp_c− are concentrated in the east and south of the TRSR. Moreover, the areas of Sol_sn_c+, Tem_sp_c+ and Pre_sn_c− also account for a smaller proportion (5.56%, 5.41% and 3.34%, respectively). These results suggest that the variation in solar radiation in the TRSR has the most extensive influence on NPP. Around the 21st century, solar radiation initially increases and then decreases; such shift in solar radiation trend is the key reason for the change from positive to negative contribution of climate factors to NPP trend.

3.2.3. Contributions of driving factors to interannual variation in NPP

Based on the results in the previous sections, the total contributions made by climate factors and *UF* are obtained, as shown in Fig. 10.

In 1982–2000 (top row of Fig. 10), the rate of interannual variation in NPP is 1.99 g cm^{-2} yr^{-2}, of which 2.47 g cm^{-2} yr^{-2} is contributed by climate and −0.48 g cm^{-2} yr^{-2} by *UF*. Climate makes a positive contribution to NPP trend in most parts of the TRSR, with higher contribution in the east than in the west. However, *UF* seems to make a negative

contribution to NPP trend. In most regions, *UF* makes a negative contribution to NPP trend, with higher contribution in the east than in the west.

In 2001–2012 (middle row of Fig. 10), the rate of interannual variation in NPP is −0.23 g cm^{-2} yr^{-2}, of which −0.78 g cm^{-2} yr^{-2} is made by climate and 0.55 g cm^{-2} yr^{-2} by *UF*. The climate factors make a strong negative contribution to NPP trend in the east of the source region of the Yellow River and in the southeast of the source regions of the Lantsang River and the Yangtze River. In the north of the source region of the Yellow River and in the middle of the source region of the Yangtze River, a strong positive contribution is made by climate factors.

At the 31-year time scale (bottom row of Fig. 10), the rate of interannual variation in NPP is 1.31 g cm^{-2} yr^{-2}, of which 1.40 g cm^{-2} yr^{-2} is made by climate factors and −0.09 g cm^{-2} yr^{-2} by *UF*. Climate factors make a positive contribution to NPP trend in most parts of the source region of the Yellow River and a negative contribution in the southwest of the TRSR. *UF* makes an intensive positive contribution in the east of the source region of the Yellow River and the south of the Lantsang River. The regions where *UF* makes a strong negative contribution are scattered in the middle and eastern parts of the TRSR.

4. Discussion

This study analyzed the spatiotemporal dynamics of NPP across different periods around the 21st century, and the characteristics of different river sources were compared. The results provided a new understanding
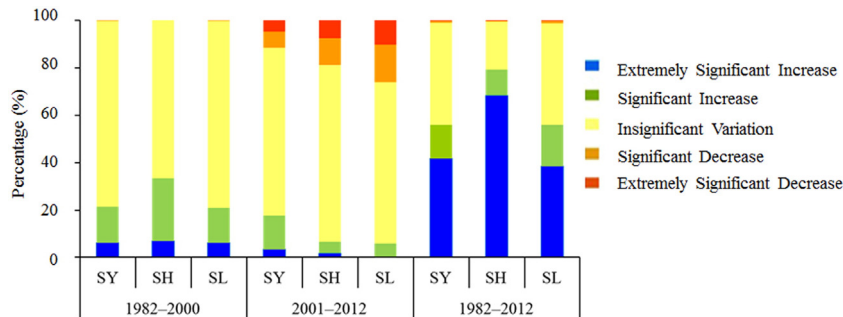

Fig. 6. Area percentages of changes in NPP at different significant levels in each river source. SY (source region of the Yangtze River), SH (source region of the Yellow River), and SL (source region of the Lantsang River).
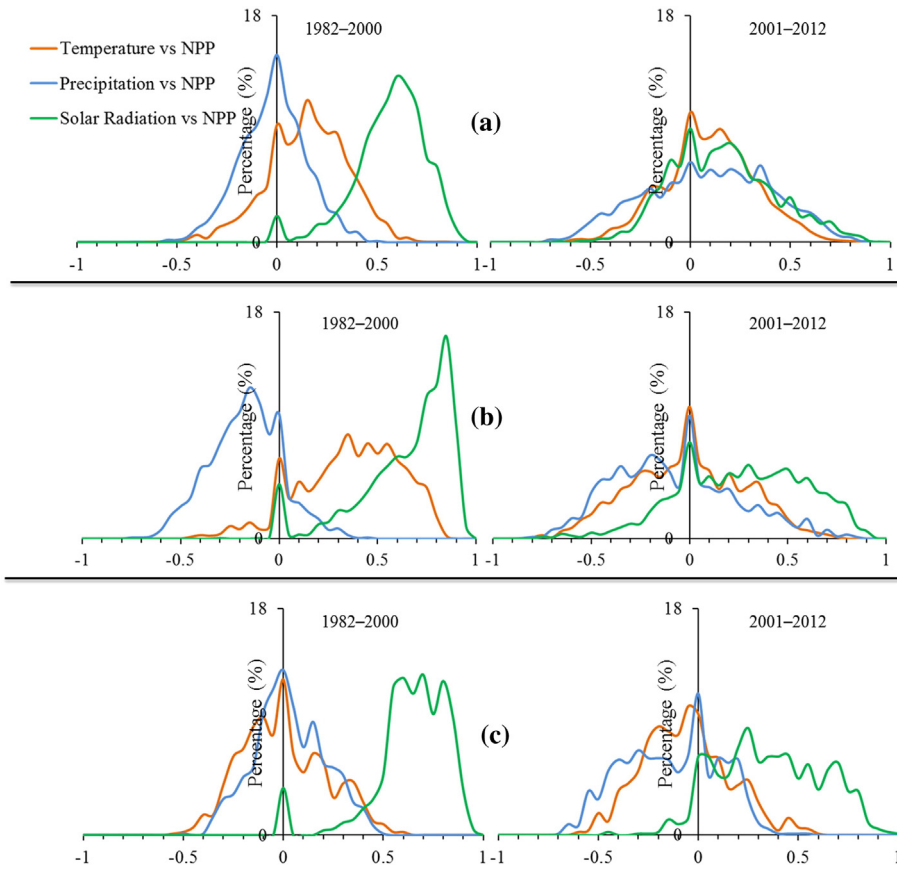
Fig. 7. Frequency by pixels of correlation coefficient between climate factors and annual NPP in each river source in two periods, i.e., 1982–2000 and 2001–2012. Source region of (a) the Yangtze River, source region of (b) the Yellow River, and source region of (c) the Lantsang River.
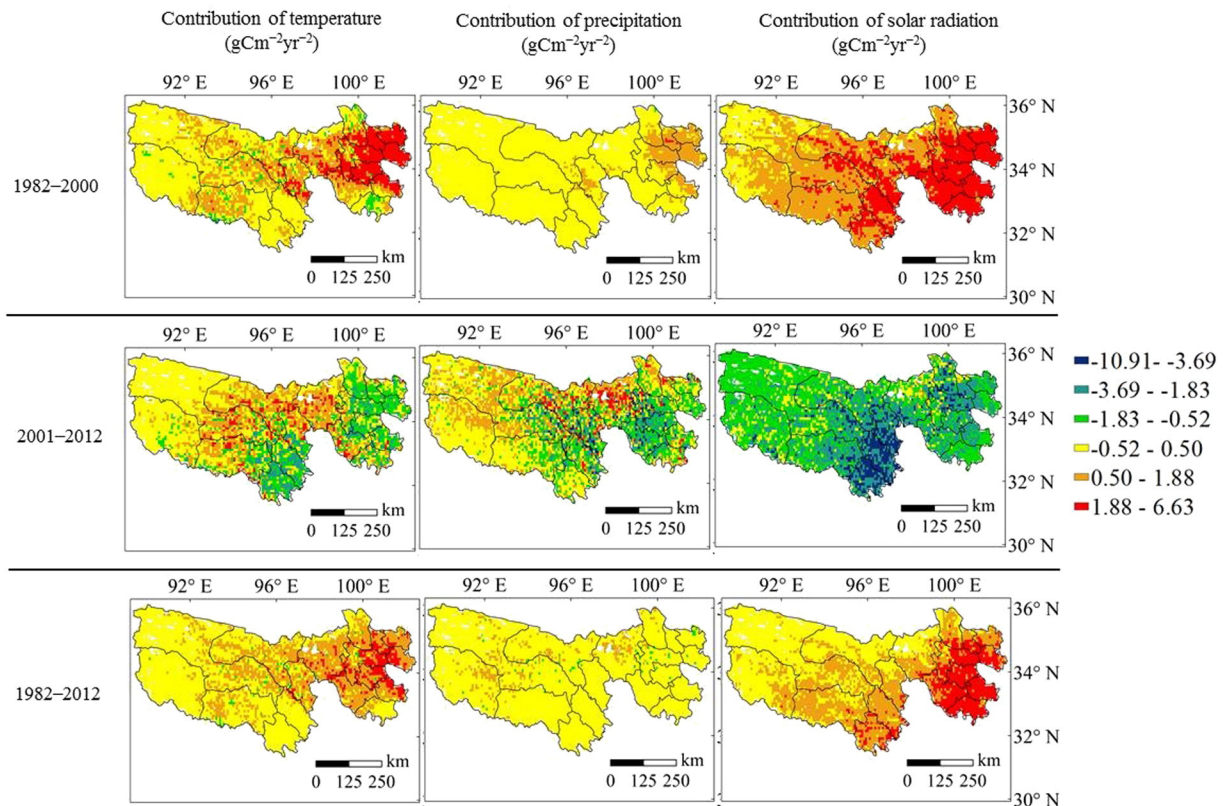

Fig. 8. Contribution of climate factors to interannual variation in NPP in different periods in the TRSR.

Table 1
Combinations of the responses of NPP to climate factors.

Combination name	Between	Partial correlation coefficient (P < 0.05)	Contribution	Meaning
Tem_sp_c+	NPP and temperature	Positive	Positive	NPP increase induced by increasing temperature
Tem_sp_c−	NPP and temperature	Positive	Negative	NPP decrease induced by decreasing temperature
Tem_sn_c+	NPP and temperature	Negative	Positive	NPP increase induced by decreasing temperature
Tem_sn_c−	NPP and temperature	Negative	Negative	NPP decrease induced by increasing temperature
Pre_sp_c+	NPP and precipitation	Positive	Positive	NPP increase induced by increasing precipitation
Pre_sp_c−	NPP and precipitation	Positive	Negative	NPP decrease induced by decreasing precipitation
Pre_sn_c+	NPP and precipitation	Negative	Positive	NPP increase induced by decreasing precipitation
Pre_sn_c−	NPP and precipitation	Negative	Negative	NPP decrease induced by increasing precipitation
Sol_sp_c+	NPP and solar radiation	Positive	Positive	NPP increase induced by increasing solar radiation
Sol_sp_c−	NPP and solar radiation	Positive	Negative	NPP decrease induced by decreasing solar radiation
Sol_sn_c+	NPP and solar radiation	Negative	Positive	NPP increase induced by decreasing solar radiation
Sol_sn_c−	NPP and solar radiation	Negative	Negative	NPP decrease induced by increasing solar radiation

of vegetation dynamics in the TRSR in recent decades. In this study, vegetation NPP exhibited an increasing trend in the typical region of the TRSR from 1982 to 2012. By contrast, several previous studies found that vegetation had been degraded at different levels in the TRSR in recent decades (Liu et al., 2006; Yang et al., 2006). Moreover, some studies showed that vegetation decreased in some regions but increased in others in recent decades (Liu et al., 2008b; Wang et al., 2008; Xu et al., 2008). These results indicated that selecting different study areas and time intervals can result in varying conclusions (Xu et al., 2011). In 1982–2012, the vegetation of the Yellow River, the Yangtze River, and the Lantsang River source regions all exhibited a generally recovering trend, with the Yellow River source region showing the biggest recovery trend; such results are similar to those of previous research (Zhang et al., 2014).

Climate change and human activities are the two major factors that affect vegetation dynamics, particularly in high-altitude regions, which are characterized by extremely fragile ecosystems. The present study showed that the relationships among different driving factors and NPP across different periods had varying characteristics. However, a general agreement that the Tibetan Plateau is particularly sensitive to global climate change exists (Cheng and Wu, 2007; Wang et al., 2007a). To detect climate change, changes in temperature, precipitation, and solar radiation during the growth season in 1982–2012 were calculated based on the climate data collected from climate stations across the TRSR.

Fig. 11 shows the temporal variations in meteorological variables during the growth season in the TRSR. The average temperature of the TRSR during the growth season in 1982–2012 was 4.60 °C, precipitation

was 358.93 mm, and solar radiation was 3111.33 MJ m^{-2}. At the 31-year time scale, temperature, precipitation, and solar radiation during the growth season all exhibited an increasing trend, with an increase rate of 0.08 °C yr^{-2}, 2.75 mm yr^{-2}, and 11.92 MJ m^{-2} yr^{-2}, respectively.

Before 2001, the regions with rapid temperature increase were distributed in the east of the source region of the Yellow River, where NPP exhibited an obvious increasing trend. By contrast, temperature increase slowed down during the growth season after 2001. Although climate warming was aggravated after the 21st century in the TRSR, such warming was mainly contributed by higher temperatures during winter (Xu et al., 2011; Liang et al., 2013). Harris (2010) suggested that vegetation was least affected by temperature when it was dormant in winter compared with other growth stages in the Qinghai–Tibetan Plateau.

Scholars have researched on the response of vegetation to climate change in the TRSR, and the results are different according to vegetation types and climate conditions of the study area. Hu et al. (2011) found that water and heat were the limiting conditions to vegetation growth, and that water was more important than heat. Other studies, however, found that the effect of temperature on vegetation was considerably more than that of moisture in this region (Yang et al., 2005; Xu et al., 2011), which is consistent with our results. The climate in the TRSR is characterized by relatively abundant precipitation and lower temperature, which indicates that the effect of moisture on vegetation in this region is significantly less than that of temperature (Xu et al., 2011). Karnieli et al. (2010) found that when energy was the limiting factor for vegetation growth in the North American continent at higher latitudes and elevations, a positive correlation existed between land surface temperature and NDVI, which is also consistent with our results. Our study also showed that precipitation mostly made negative contributions to NPP trend in the eastern and middle parts of the TRSR after the 21st century, which indicated that precipitation condition in this region was unfavorable for vegetation growth during this period. The correlation coefficient during this period indicated a negative correlation between NPP and precipitation in this region, particularly in the southeast area. This result also agrees well with Gao et al.'s (2013) study on the Tibetan plateau because an increase in precipitation caused a decrease in temperature and radiation, which inhibited photosynthesis in plants, while precipitation also increases soil erosion to some extent, which decreases the soil organic matter content, thus reducing productivity. Furthermore, our study showed that the factor that restricted NPP growth changed from temperature and radiation to precipitation after the 21st century in the TRSR, on the whole. We also found that solar radiation was the key influential factor of interannual variation in NPP in each period. Although the TRSR has abundant solar energy resource, the distribution of solar energy is not uniform, and the influences from monsoon and altitudinal gradient are significant. Solar energy decreases from northwest to southeast. Solar radiation serves as an important energy source for the photosynthesis of plants. According to Nemani et al. (2003), the largest global increase in NPP is mainly attributed to the
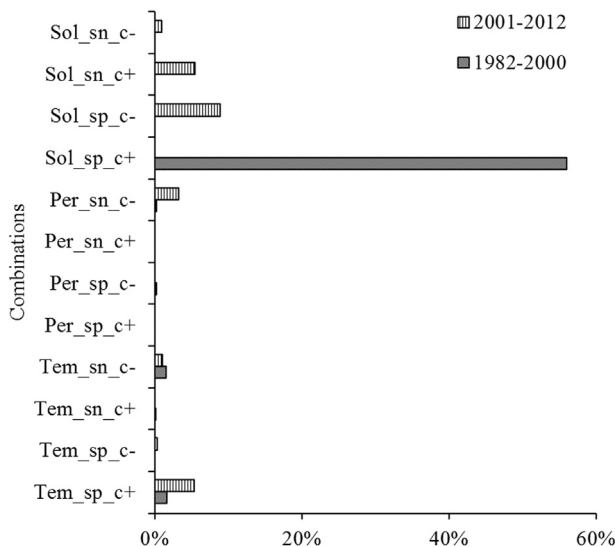

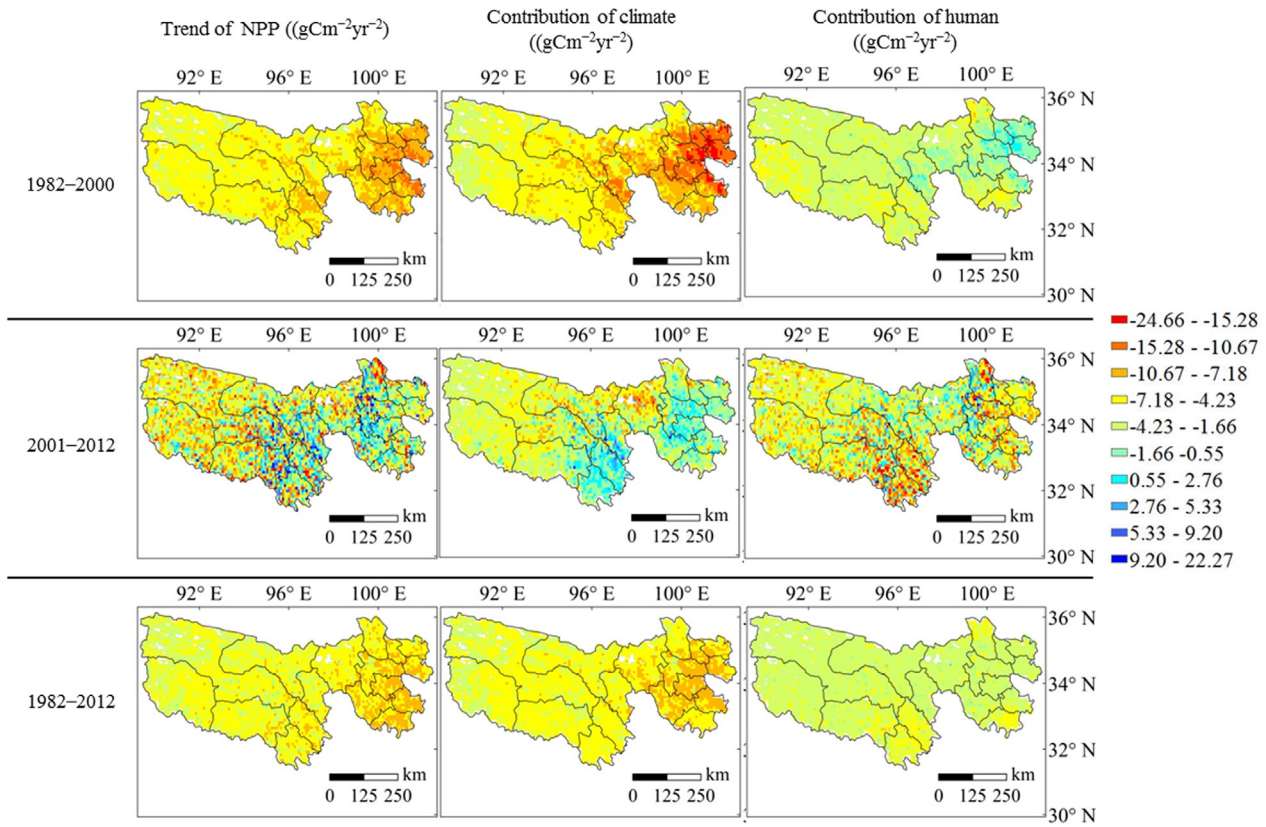**Fig. 9.** Responses of NPP to climatic variation trends.

Fig. 10. Interannual variation trends of NPP and the contributions of climate factors and *UF* to NPP trend during different periods in the TRSR.

decrease in cloud cover and the resulting increase in solar radiation. Piao et al. (2006) showed that solar radiation exerted a larger influence on vegetation NPP in the Tibetan Plateau compared with temperature and precipitation.

Overall, given the increases in temperature and radiation in 1982–2001, as well as the decrease in radiation in 2001 to 2012, the general climate condition in the TRSR changed from vegetation growth-conducive to growth-hostile at the turn of the century.

As previously mentioned, both human factors and some natural factors are contained in the *UF*. Some of these environmental factors (such as vegetation type and soil texture) are relatively stable on the time scale, and their effect on NPP interannual variation can be neglected.
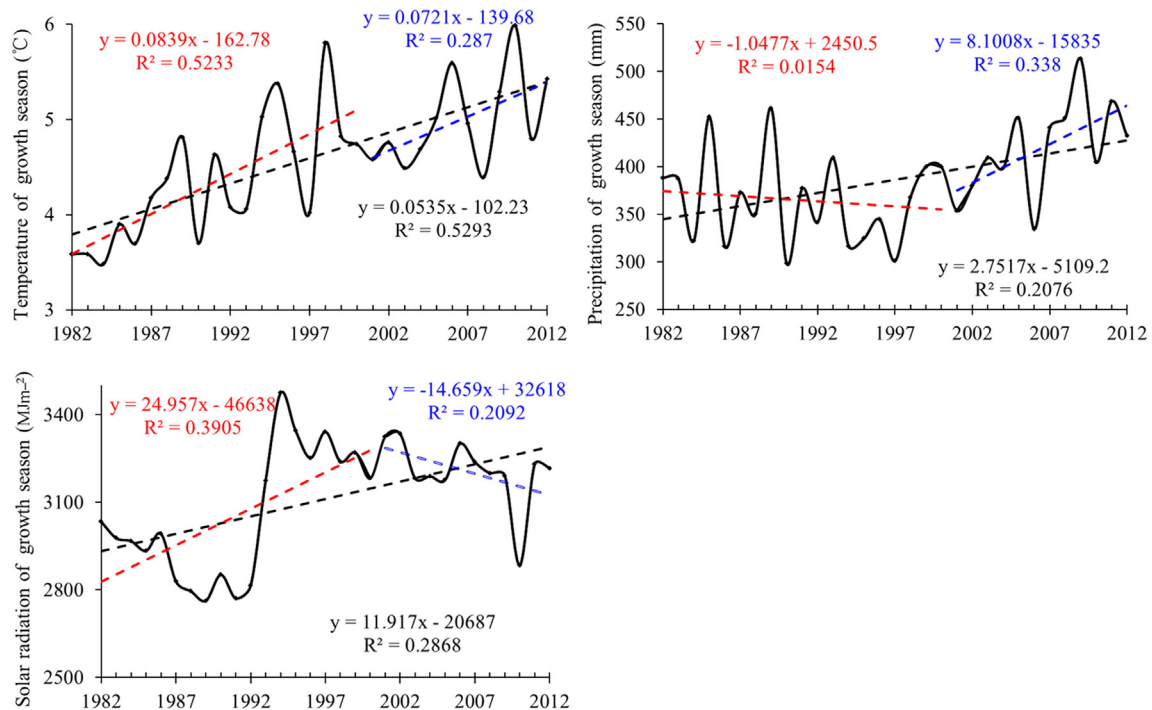

Fig. 11. Temporal variations in meteorological variables during the growth season in the TRSR. (a) Average temperature, (b) precipitation, (c) solar radiation.

Rodent pests significantly affect vegetation degradation in the TRSR. Given that one of the dominant causes of rodent infestation is overgrazing and rodent pest control is an important part of grassland recovery measures (Fang, 2013), this factor could be considered as an anthropogenic factor. The atmospheric CO^2 factor is also likely to be included in *UF*. Although CO_2 fertilization could have a strong impact on the Chinese carbon sink (Fang et al., 2003), its impact on grasslands is the weakest and only accounts for 0.3% of the total NPP (Mu et al., 2008). Sui et al. (2013) reported that the impacts of CO_2 concentration was obviously slighter than other climatic factors on carbon storage of grassland ecosystems. Therefore, we suppose that anthropogenic factors play a crucial role in *UF* in the TRSR. Moreover, *UF* can be used to evaluate the influence of human activities.

A grassland degradation pattern had already formed in the TRSR in the 1970s (Liu et al., 2008b). The residents of this region are mostly Tibetans, who rely on grazing as their major source of income; however, the educational and grazing methods of the residents are not too developed (Fang, 2013). Given the pursuit of short-term benefits of the residents as well as the lack of effective protection and management measures during the 1980s and 1990s, vegetation degradation was aggravated artificially in some areas of the TRSR through overgrazing, unreasonable farming, wood harvesting, collection of Chinese herbal medicines, and gold mining (Wang and Cheng, 2000; Ren and Lin, 2005; Fan et al., 2010), with overgrazing as the most important reason (Ren and Lin, 2005). Fan et al. (2010) pointed out that Tongde County, Zeku County, and Henan County in the east of the TRSR suffered from the largest grazing pressure before 2001, and our study also revealed that human activities produced the greatest negative impact in these regions during the same period. However, the general climate conditions in this period were favorable to vegetation recovery, and the influence of climate conditions was larger than that of human activities. Thus, vegetation recovery was significant before 2001. After 2001, NPP decreased in the TRSR primarily because of deteriorating climate conditions. However, the influence of human activities was enhanced, and the negative contribution of human activities to NPP trend before 2001 changed into a positive contribution after 2001, which counteracted the negative influence of climate conditions on vegetation NPP during this period. This result agrees well with the finding of the study of Chen et al. (2014) on the Tibetan Plateau. The Three-River Source Nature Reserve was designated in 2000 and it became the largest national nature reserve in China in 2003. Major ecological protection projects and constructions, such as GTGP, GWP, ecological immigration, treatment of "Black Beach," and rodent pest control, were launched in the TRSR to facilitate ecological restoration and degradation control (Fang, 2013). A certain efficacy was achieved (Fan et al., 2010; Liu et al., 2014; Tong et al., 2014). Thus, human activities produced a favorable impact on vegetation recovery during this period.

At the 31-year time scale, climate conditions were generally favorable for vegetation growth, whereas human activities produced a negative impact. As shown by the absolute values of the contributions made by climate and human activities, the influence on the interannual variation in NPP of climate factors was always larger than that of human activities in all periods. Given that the TRSR is located in the hinterland of the Tibetan Plateau, population is sparse in this region and human activities are less intense. A considerable proportion of grassland cannot be utilized or is rarely utilized in this region. Notably, the effect of some protection projects is less than satisfactory. Looking forward, the effectiveness of restoration projects should be further adjusted to balance environmental conservation and economic development. More plausible adaptation strategies should be employed to cope with climate change.

However, there are still some driving factors (such as wind, N deposition) of NPP dynamics that have not been considered in this study. Our understanding of the effects of different driving forces on vegetation dynamics is still limited by available data and experimental proof. It is very necessary for us to further study how to separately quantify the influence of climatic and anthropogenic factors more effectively and establish the quantitative effects of different human activities.

5. Conclusions

From 1982 to 2012, the average NPP in the TRSR demonstrated a fluctuation but presented a generally increasing trend. The increase rate was 1.31 g cm^{-2} yr^{-1}. NPP increased significantly in 62.87% of the total area, and the proportion of areas with NPP increase was the largest in the source region of the Yellow River. Before 2001, NPP increase over the entire TRSR was fast. The source region of the Yellow River had the largest proportion of areas with an increase in NPP. After 2001, NPP over the entire TRSR did not decrease considerably. The source region of the Lantsang River had the highest proportion of areas with a reduction in NPP.

During the entire study period, the average contributions of temperature, precipitation, and radiation to NPP interannual variation over the whole region were 0.58, 0.73, and 0.09 g cm^{-2} yr^{-2}, respectively. Solar radiation was the climate factor with the greatest influence on interannual variation in NPP. The comparison before and after 2001 showed that the factor that restricted the increase in NPP changed from temperature and radiation to precipitation. Overall, given the increases in temperature and radiation during 1982–2001, and the decrease in radiation during 2001–2012, the general climate condition of the TRSR changed from vegetation growth-conducive to growth-hostile by the turn of the century.

During the entire study period, the average contributions of climate change and human activities to NPP interannual variation over the whole region were 1.40 g cm^{-2} yr^{-2} and −0.08 g cm^{-2} yr^{-2}, respectively. Before 2001, human activities had a negative impact on vegetation growth. After 2001, however, human activities made a favorable impact on vegetation recovery.

References

Akiyama, T., Kawamura, K., 2007. Grassland degradation in China: methods of monitoring, management and restoration. Grassl. Sci. 53, 1–17.

An, R., Xu, X.F., Yang, R.M., 2014. Time-lag effect of vegetation NDVI on regional climate in "Three River Source" region. Geomat. Spatial Inform. Technol. 37, 1–5 (in Chinese, with English abstract).

Chang, X.F., Wang, S.P., Cui, S.J., Zhu, X.X., Luo, C.Y., Zhang, Z.H., Wilkes, A., 2014. Alpine grassland soil organic carbon stock and its uncertainty in the Three Rivers Source Region of the Tibetan Plateau. PLoS One 9, 1–10 e97140.

Chen, B.X., Zhang, X.Z., Tao, J.S., Wu, J.S., Wang, J.S., Shi, P.L., et al., 2014. The impact of climate change and anthropogenic activities on alpine grassland over the Qinghai–Tibet Plateau. Agric. For. Meteorol. 189, 11–18.

Cheng, G.D., Wu, T.H., 2007. Responses of permafrost to climate change and their environmental significance, Qinghai–Tibet Plateau. J. Geophys. Res. Earth Surf. 112, 1–10, F02S03.

Esser, G., 1987. Sensitivity of global carbon pools and fluxes to human and potential climatic impacts. Tellus B 39, 245–260.

Fan, J.W., Shao, Q.Q., Liu, J.Y., Wang, J.B., Harris, W., Chen, Z.Q., et al., 2010. Assessment of effects of climate change and grazing activity on grassland yield in the Three Rivers Headwaters Region of Qinghai–Tibet Plateau, China. Environ. Monit. Assess. 170, 571–584.

Fang, Y.P., 2013. Managing the Three-Rivers Headwater Region, China: from ecological engineering to social engineering. Ambio 42, 566–576.

Fang, J., Piao, S., Field, C.B., Pan, Y., Guo, Q., Zhou, L., et al., 2003. Increasing net primary production in China from 1982 to 1999. Front. Ecol. Environ. 1, 293–297.

Field, C.B., Randerson, J.T., Malmstrom, C.M., 1995. Global net primary production — combining ecology and remote-sensing. Remote Sens. Environ. 51, 74–88.

Field, C.B., Behrenfeld, M.J., Randerson, J.T., Falkowski, P., 1998. Primary production of the biosphere: integrating terrestrial and oceanic components. Science 281, 237–240.

Foggin, J.M., 2008. Depopulating the Tibetan grasslands - National policies and perspectives for the future of Tibetan herders in Qinghai Province. China. Mt. Res. Dev. 28, 26–31.

Gao, Q.Z., Li, Y., Wan, Y.F., Qin, X.B., Jiangcun, W.Z., Liu, Y.H., 2009. Dynamics of alpine grassland NPP and its response to climate change in Northern Tibet. Clim. Chang. 97, 515–528.

Gao, Y.H., Zhou, X., Wang, Q., Wang, C.Z., Zhan, Z.M., Chen, L.F., et al., 2013. Vegetation net primary productivity and its response to climate change during 2001–2008 in the Tibetan Plateau. Sci. Total Environ. 444, 356–362.

Haberl, H., 1997. Human appropriation of net primary production as an environmental indicator: implications for sustainable development. Ambio 26, 143–146.

Harris, R.B., 2010. Rangeland degradation on the Qinghai–Tibetan plateau: a review of the evidence of its magnitude and causes. J. Arid Environ. 74, 1–12.

Hein, L, De Ridder, N., Hiernaux, P., Leemans, R., De Wit, A., Schaepman, M., 2011. Desertification in the Sahel: towards better accounting for ecosystem dynamics in the interpretation of remote sensing images. J. Arid Environ. 75, 1164–1172.

Hu, M.Q., Mao, F., Sun, H., Hou, Y.Y., 2011. Study of normalized difference vegetation index variation and its correlation with climate factors in the Three-River-Source Region. Int. J. Appl. Earth Obs. Geoinf. 13, 24–33.

Hutchinson, M., 2001. ANUSPLIN Version 4.2 User Guide. Centre for Resource and Environmental Studies, Australian National University, Canberra.

IPCC, 2007. Climate Change 2007: the physical science basis. Contribution of Working Group I to the Fourth Assessment Report of the Intergovernmental Panel on Climate Change (United Kingdom/NewYork, NY, USA).

Karnieli, A., Agam, N., Pinker, R.T., Anderson, M., Imhoff, M.L., Gutman, G.G., 2010. Use of NDVI and Land Surface Temperature for Drought Assessment: Merits and Limitations. J. Clim. 23, 618–633.

Li, X., Cheng, G., Lu, L., 2003. Comparison study of spatial interpolation methods of air temperature over Qinghai–Xizang Plateau. Plateau Meteor. 26, 565–573 (in Chinese, with English abstract).

Liang, L.Q., Li, L.J., Liu, C.M., Cuo, L., 2013. Climate change in the Tibetan Plateau Three Rivers Source Region: 1960–2009. Int. J. Climatol. 33, 2900–2916.

Liu, L.S., Zhang, Yl, Bai, W.Q., 2006. Characteristics of grassland degradation and driving forces in the source region of the Yellow River from 1985 to 2000. J. Geogr. Sci. 16, 131–142.

Liu, J.G., Li, S.X., Ouyang, Z.Y., Tam, C., Chen, X.D., 2008a. Ecological and socioeconomic effects of China's policies for ecosystem services. Proc. Natl. Acad. Sci. U. S. A. 105, 9477–9482.

Liu, J.Y., Xu, X.L., Shao, Q.Q., 2008b. Grassland degradation in the "Three-River Headwaters" Region, Qinghai Province. J. Geogr. Sci. 18, 259–273.

Liu, X.F., Zhang, J.S., Zhu, X.F., Pan, Y.Z., Liu, Y.X., Zhang, D.H., et al., 2014. Spatiotemporal changes in vegetation coverage and its driving factors in the Three-River Headwaters Region during 2000–2011. J. Geogr. Sci. 24, 288–302.

Meng, D.J., Mo, X.G., 2012. Assessing the effect of climate change on mean annual runoff in the Songhua River basin, China. Hydrol. Process. 26, 1050–1061.

Mu, Q., Zhao, M., Running, S.W., Liu, M., Tian, H., 2008. Contribution of increasing CO_2 and climate change to the carbon cycle in China's ecosystems. J. Geophys. Res. Biogeosci. 113.

Mu, S.J., Chen, Y.Z., Li, J.L., Ju, W.M., Odeh, I.O.A., Zou, X.L., 2013a. Grassland dynamics in response to climate change and human activities in Inner Mongolia, China between 1985 and 2009. Rangel. J. 35, 315–329.

Mu, S.J., Zhou, S.X., Chen, Y.Z., Li, J.L., Ju, W.M., Odeh, I.O.A., 2013b. Assessing the impact of restoration-induced land conversion and management alternatives on net primary productivity in Inner Mongolian grassland, China. Glob. Planet. Chang. 108, 29–41.

Nayak, R., Patel, N., Dadhwal, V., 2013. Inter-annual variability and climate control of terrestrial net primary productivity over India. Int. J. Climatol. 33, 132–142.

Nemani, R.R., Keeling, C.D., Hashimoto, H., Jolly, W.M., Piper, S.C., Tucker, C.J., et al., 2003. Climate-driven increases in global terrestrial net primary production from 1982 to 1999. Science 300, 1560–1563.

Peng, H., Liu, F., Duo, H., Li, D., 2010. Conpartion of spatial interpolation methods on temperature and precipitation of San Jiangyuan region. J. Anhui Agri. 38, 9646–9649.

Piao, S.L., Fang, J.Y., He, J.S., 2006. Variations in vegetation net primary production in the Qinghai–Xizang Plateau, China, from 1982 to 1999. Clim. Chang. 74, 253–267.

Potter, C.S., Randerson, J.T., Field, C.B., Matson, P.A., Vitousek, P.M., Mooney, H.A., Klooster, S.A., 1993. Terrestrial ecosystem production: a process model based on global satellite and surface data. Glob. Biogeochem. Cycles 7, 811–841.

Qian, S., Fu, Y., Pan, F.F., 2010. Climate change tendency and grassland vegetation response during the growth season in Three-River Source Region. Sci. Sin. Terrae 40, 1439–1445.

Rana, G., Katerji, N., 1998. A measurement based sensitivity analysis of the Penman–Monteith actual evapotranspiration model for crops of different height and in contrasting water status. Theor. Appl. Climatol. 60, 141–149.

Ren, J.Z., Lin, H.L., 2005. Assumed plan on grassland ecological reconstruction in the source region of Yangtse River, Yellow River and Lantsang River. Acta Pratacult. Sci. 14, 1–8 (in Chinese, with English abstract).

Ruimy, A., Saugier, B., Dedieu, G., 1994. Methodology for the estimation of terrestrial net primary production from remotely sensed data. J. Geophys. Res.-Atmos. 99, 5263–5283.

Sui, X.H., Zhou, G.S., Zhuang, Q.L., 2013. Sensitivity of carbon budget to historical climate variability and atmospheric CO2 concentration in temperate grassland ecosystems in China. Clim. Change 117, 259–272.

Tong, L., Xu, X.L., Fu, Y., Li, S., 2014. Wetland changes and their responses to climate change in the "Three-River Headwaters" region of China since the 1990s. Energies 7, 2515–2534.

Vitousek, P.M., 1994. Beyond global warming: ecology and global change. Ecology 75, 1861–1876.

Wang, G.X., Cheng, G.D., 2000. Eco-environmental changes and causative analysis in the source regions of the Yangtze and Yellow Rivers, China. Environmentalist 20, 221–232.

Wang, G.X., Wang, Y.B., Li, Y.S., Cheng, H.Y., 2007a. Influences of alpine ecosystem responses to climatic change on soil properties on the Qinghai–Tibet Plateau, China. Catena 70, 506–514.

Wang, X.H., Lu, C.H., Fang, J.Y., Shen, Y.C., 2007b. Implications for development of grain-for-green policy based on cropland suitability evaluation in desertification-affected north China. Land Use Policy 24, 417–424.

Wang, L.W., Wei, Y.X., Niu, Z., 2008. Spatial and temporal variations of vegetation in Qinghai Province based on satellite data. J. Geogr. Sci. 18, 73–84.

Wang, J.B., Liu, J.Y., Shao, Q.Q., Liu, R.G., Fan, J.W., Chen, Z.Q., 2009. Spatial-temporal patterns of net primary productivity for 1988–2004 based on GLOPEM–CEVSA model in the "Three-River Headwaters" region of QingHai Province, China. Chin. J. Plant Ecol. 33, 254–269 (in Chinese, with English abstract).

Wessels, K., Prince, S., Frost, P., Van Zyl, D., 2004. Assessing the effects of human-induced land degradation in the former homelands of northern South Africa with a 1 km AVHRR NDVI time-series. Remote Sens. Environ. 91, 47–67.

Wu, Y., Tan, H.C., Deng, Y.C., Wu, J., Xu, X.L., Wang, Y.F., et al., 2010. Partitioning pattern of carbon flux in a Kobresia grassland on the Qinghai–Tibetan Plateau revealed by field ^{13}C pulse-labeling. Glob. Chang. Biol. 16, 2322–2333.

Wu, S.H., Zhou, S.L., Chen, D.X., Wei, Z.Q., Dai, L., Li, X.G., 2014. Determining the contributions of urbanisation and climate change to NPP variations over the last decade in the Yangtze River Delta, China. Sci. Total Environ. 472, 397–406.

Xu, X.K., Chen, H., Levy, J.K., 2008. Spatiotemporal vegetation cover variations in the Qinghai–Tibet Plateau under global climate change. Chin. Sci. Bull. 53, 915–922.

Xu, W.X., Gu, S., Zhao, X.Q., Xiao, J.S., Tang, Y.H., Fang, J.Y., et al., 2011. High positive correlation between soil temperature and NDVI from 1982 to 2006 in alpine meadow of the Three-River Source Region on the Qinghai–Tibetan Plateau. Int. J. Appl. Earth Obs. Geoinf. 13, 528–535.

Yang, H.B., Yang, D.W., 2012. Climatic factors influencing changing pan evaporation across China from 1961 to 2001. J. Hydrol. 414, 184–193.

Yang, D.W., Ding, F., Chen, B.X., 2005. NDVI reflection of alpine vegetation changes in the source regions of the Yangtze and Yellow Rivers. Acta Geograph. Sin. 60, 467–478 (in Chinese, with English abstract).

Yang, J.P., Ding, Y.J., Chen, R.S., 2006. Spatial and temporal of variations of alpine vegetation cover in the source regions of the Yangtze and Yellow Rivers of the Tibetan Plateau from 1982 to 2001. Environ. Geol. 50, 313–322.

Yang, H.F., Mu, S.J., Li, J.L., 2014. Effects of ecological restoration projects on land use and land cover change and its influences on territorial NPP in Xinjiang, China. Catena 115, 85–95.

Yu, D.Y., Shi, P.J., Shao, H.B., Zhu, W.Q., Pan, Y.Z., 2009. Modelling net primary productivity of terrestrial ecosystems in East Asia based on an improved CASA ecosystem model. Int. J. Remote Sens. 30, 4851–4866.

Yu, D.Y., Shi, P.J., Han, G.Y., Zhu, W.Q., Du, S.Q., Xun, B., 2011. Forest ecosystem restoration due to a national conservation plan in China. Ecol. Eng. 37, 1387–1397.

Zhang, Y.Y., Zhang, S.F., Zhai, X.Y., Xia, J., 2012. Runoff variation and its response to climate change in the Three Rivers Source Region. J. Geogr. Sci. 22, 781–794.

Zhang, Y.L., Qi, W., Zhou, C.P., Ding, M.J., Liu, L.S., Gao, J.G., et al., 2014. Spatial and temporal variability in the net primary production of alpine grassland on the Tibetan Plateau since 1982. J. Geogr. Sci. 24, 269–287.

Zhou, W., Gang, C.C., Zhou, F.C., Li, J.L., Dong, X.G., Zhao, C.Z., 2015. Quantitative assessment of the individual contribution of climate and human factors to desertification in northwest China using net primary productivity as an indicator. Ecol. Indic. 48, 560–569.

Zhu, W.Q., Pan, Y.Z., Zhang, J.S., 2007. Estimation of net primary productivity of Chinese terrestrial vegetation based on remote sensing. J. Plant Ecol. 31, 413–424 (in Chinese, with English abstract).